Plasma Expansion into a Vacuum

P. Mora

Centre de Physique Théorique (UMR 7644 du CNRS), Ecole Polytechnique, Palaiseau 91128 Cedex, France

(Received 27 September 2002; published 7 May 2003)

The charge separation effects in the collisionless plasma expansion into a vacuum are studied in great detail. Accurate results are obtained concerning the structure of the ion front, the resultant ion energy spectrum, and more specifically the maximum ion energy. These are of crucial importance for the interpretation of recent experiments, where high-energy ion jets were produced from short pulse interaction with solid targets.

DOI: 10.1103/PhysRevLett.90.185002 PACS numbers: 52.38.Kd, 41.75.Jv, 52.40.Kh, 52.65.–y

Recent experiments producing high-energy ion jets from short-pulse interaction with solid targets [1–11] have renewed the interest in models of free plasma expansion into a vacuum [12–24]. Of particular interest is the ion spectrum and the maximum ion energy obtained in the experiments. Though widely used in the interpretation of the experimental results, the freely expanding plasma model has not been fully explored in terms of charge separation effects and structure of the ion front, which are still a matter of controversy [20]. Usually simple estimates are given while we demonstrate in this Letter that very accurate results can be obtained.

We first recall the fundamentals of the model. At time $t = 0$, a plasma is assumed to occupy the half-space $x < 0$. The ions are cold and initially at rest with density $n_i = n_{i0}$ for $x < 0$ and $n_i = 0$ for $x > 0$ with a sharp boundary. On the other hand the electron density n_e is continuous and corresponds to a Boltzmann distribution,

$$n_e = n_{e0} \exp(e\Phi/k_B T_e), \tag{1}$$

where n_{e0} is the electron density in the unperturbed plasma (i.e., for $x = -\infty$), Φ is the electrostatic potential, and T_e is the electron temperature, which may be in the relativistic domain. [In (1) and in following equations, e is the elementary charge, with the exception of Eqs. (3), (9), (11), and (13) below, where e denotes the numerical constant 2.718 28 ....] One has $\Phi(-\infty) = 0$ and $n_{e0} = Zn_{i0}$, where Z is the ion charge number. The potential Φ satisfies the Poisson equation,

$$\epsilon_0 \partial^2 \Phi/\partial x^2 = e(n_e - Zn_i). \tag{2}$$

A simple expression for the electric field at $x = 0$ is obtained by integration of the Poisson equation from $x = 0$ to $x = \infty$ [13],

$$E_{\text{front},0} = \sqrt{2/e} E_0, \tag{3}$$

where $E_0 = (n_{e0} k_B T_e/\epsilon_0)^{1/2}$. The initial condition corresponds exactly to Figs. 1 of [13,17].

For $t > 0$ the electrons are assumed to stay in equilibrium with the potential Φ [16], so that Eqs. (1) and (2) still hold, while the ion expansion into a vacuum is described by the equations of continuity and motion,

$$(\partial/\partial t + v_i \partial/\partial x) n_i = -n_i \partial v_i/\partial x, \tag{4}$$

$$(\partial/\partial t + v_i \partial/\partial x) v_i = -(Ze/m_i) \partial\Phi/\partial x, \tag{5}$$

where v_i is the ion velocity. For $x + c_s t > 0$, a self-similar expansion is found if one assumes quasineutrality in the expanding plasma, with $n_e = Zn_i = n_{e0} \exp(-x/c_s t - 1)$, $v_i = c_s + x/t$, and

$$E_{\text{ss}} = k_B T_e/ec_s t = E_0/\omega_{pi} t, \tag{6}$$

where ss stands for self-similar, $c_s = (Zk_B T_e/m_i)^{1/2}$ is the ion-acoustic velocity, and $\omega_{pi} = (n_{e0} Ze^2/m_i \epsilon_0)^{1/2}$ is the ion plasma frequency. The self-similar field corresponds to a positive charge surface $\sigma = \epsilon_0 E_{\text{ss}}$ at position $x = -c_s t$ and a negative charge surface $-\sigma$ at the plasma edge.

First, the self-similar solution has no meaning as long as the initial Debye length, $\lambda_{D0} = (\epsilon_0 k_B T_e/n_{e0} e^2)^{1/2}$, is larger than the self-similar density scale length, $c_s t$, i.e., for $\omega_{pi} t < 1$. Second, for $\omega_{pi} t \gg 1$, the self-similar model predicts a velocity increasing without limit for x going to infinity. Physically the ion velocity is limited to a finite value and the ions originally at $x = 0$ form a well-defined ion front [13]. A rough estimate of the position of the ion front [14] can be obtained by noting that the self-similar solution becomes invalid when the local Debye length, $\lambda_D = \lambda_{D0}(n_{e0}/n_e)^{1/2} = \lambda_{D0} \exp[(1 + x/c_s t)/2]$, equals the density scale length, $c_s t$. This position corresponds to $1 + x/c_s t = 2 \ln(\omega_{pi} t)$ (see also Ref. [18] for a different argument). At that point the self-similar solution predicts a velocity $v_{i,\text{front}} = 2c_s \ln(\omega_{pi} t)$. Note that this implies that the electric field at the ion front is *twice* the self-similar field E_{ss},

$$E_{\text{front}} \simeq 2E_{\text{ss}} = 2E_0/\omega_{pi} t. \tag{7}$$

This is easily verified by integrating E_{ss} over time.

To ascertain these estimates and to be far more precise, we have developed a Lagrangian code which solves Eqs. (1), (2), (4), and (5). The numerical methods are similar to that described in [17]. In particular, for solving the Poisson equation (2), we use the boundary condition at

the ion front obtained by integrating the Poisson equation from $x = x_{\text{front}}$ to $x = \infty$,

$$E_{\text{front}} = \sqrt{2}E_0 \exp(e\Phi_{\text{front}}/2k_BT_e) = (2n_{e,\text{front}}/n_{e0})^{1/2}E_0 = \sqrt{2}k_BT_e/e\lambda_D. \quad (8)$$

The numerical box is limited to $x > -L$ with $L \gg c_st$ and $v_i(-L) = E(-L) = 0$.

Figure 1 shows the charge separation as a function of space at time $\omega_{pi}t = 50$, for which the ion front stands at $x/c_st \simeq 5.59$. Three distinct zones are clearly seen: a first positive layer of charge $\sigma = \epsilon_0 E_{\text{ss}}$ per unit surface around the position $x = -c_st$, where the expansion starts; a second positive layer of the same charge σ just on the left of the ion front; and a negative layer due to the electron cloud on its right, with charge -2σ. As expected, the total charge around the ion front is $-\sigma$.

The corresponding electric field is shown in Fig. 2 at the same time, showing the rapid increase of the electric field in the vicinity of the ion front.

The evolution of the electric field at the ion front is shown in Fig. 3 as a function of time. A very precise expression for the electric field at the ion front, valid for any time, is

$$E_{\text{front}} \simeq 2E_0/(2e + \omega_{pi}^2t^2)^{1/2}. \quad (9)$$

One can verify that this expression has the correct behavior both for $t = 0$ [Eq. (3)] and for $\omega_{pi}t \gg 1$ [Eq. (7)]. Moreover, the precision of this interpolation formula is of the order of a percent or less, as can be seen in Fig. 3, where one hardly distinguishes the numerical result and the curve corresponding to Eq. (9). As a result, accurate predictions can be made for the characteristics of the ion front. First of all, integrating $dv_{\text{front}}/dt = ZeE_{\text{front}}/m_i$, with E_{front} given by Eq. (9), and $dx_{\text{front}}/dt = v_{\text{front}}$, one obtains successively the ion front velocity and position as a function of time,

$$v_{\text{front}} \simeq 2c_s \ln(\tau + \sqrt{\tau^2 + 1}), \quad (10)$$

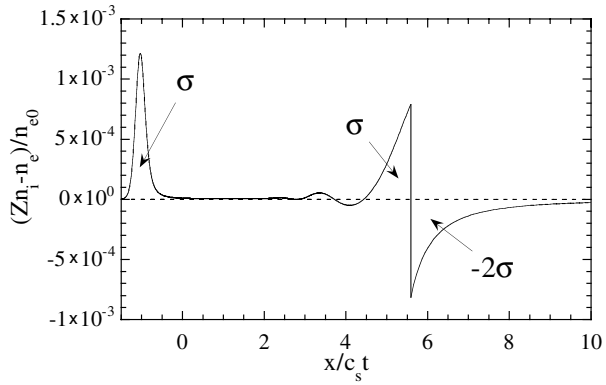

FIG. 1. Charge separation at time $\omega_{pi}t = 50$. The ion front stands at $x/c_st \simeq 5.59$.

$$x_{\text{front}} \simeq 2\sqrt{2e}\lambda_{D0}[\tau \ln(\tau + \sqrt{\tau^2 + 1}) - \sqrt{\tau^2 + 1} + 1], \quad (11)$$

where $\tau = \omega_{pi}t/\sqrt{2e}$.

In the asymptotic limit, $\omega_{pi}t \gg 1$, Eqs. (10) and (11) reduce to

$$v_{\text{front}} \simeq 2c_s \ln(2\tau) = c_s[2\ln(\omega_{pi}t) + \ln 2 - 1]. \quad (12)$$

$$x_{\text{front}} \simeq 2\sqrt{2e}\lambda_{D0}\tau[\ln(2\tau) - 1] = c_st[2\ln(\omega_{pi}t) + \ln 2 - 3]. \quad (13)$$

Figure 4 shows the maximum velocity as a function of time both from simulation and from Eq. (10). One can see the excellent agreement between the two curves.

The structure of the ion front is shown in Fig. 5 for $\omega_{pi}t = 50$ and $\omega_{pi}t = 100$ as a function of x/c_st. Also shown is the usual self-similar solution. No ion bump is observed, in contrast to the results of [13,18] but in agreement with those of [17,19].

In fact, from the equations of the model, analytical results can be derived in the asymptotic limit, $\omega_{pi}t \gg 1$, which clearly rule out the existence of an ion bump for our initial conditions. Comparison of Eqs. (8) and (9) gives immediately (for $\omega_{pi}t \gg 1$)

$$n_{e,\text{front}} \simeq 2n_{e0}/\omega_{pi}^2t^2. \quad (14)$$

We then use Eqs. (2), (4), and (5) to derive

$$\frac{d^2}{dt^2}\ln n_i - \left(\frac{d}{dt}\ln n_i\right)^2 = \omega_{pi}^2\frac{n_e - Zn_i}{n_{e0}}, \quad (15)$$

where $d/dt = \partial/\partial t + v_i\partial/\partial x$. To get this result, we used the fact that $\partial/\partial x$ and d/dt do not commute, i.e.,

$$\frac{\partial}{\partial x}\frac{d}{dt} = \left(\frac{d}{dt} + \frac{\partial v}{\partial x}\right)\frac{\partial}{\partial x} = \left(\frac{d}{dt} - \frac{d}{dt}\ln n_i\right)\frac{\partial}{\partial x}. \quad (16)$$

Applying Eq. (15) to the ion front and looking for a

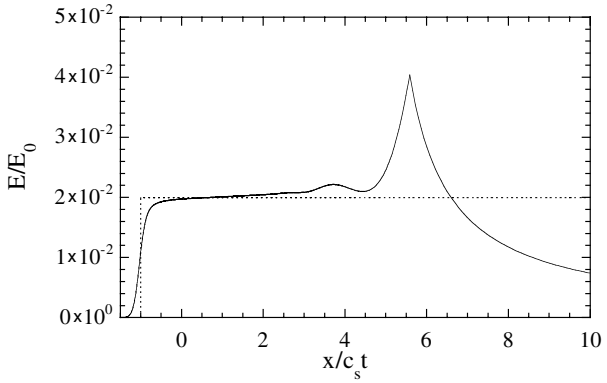

FIG. 2. Electric field at time $\omega_{pi}t = 50$. The ion front stands at $x/c_st \simeq 5.59$ where the electric field peaks. The dotted line corresponds to the usual self-similar solution, Eq. (6). Note that the electric field at the ion front is approximately twice the self-similar field, as predicted by Eq. (7).

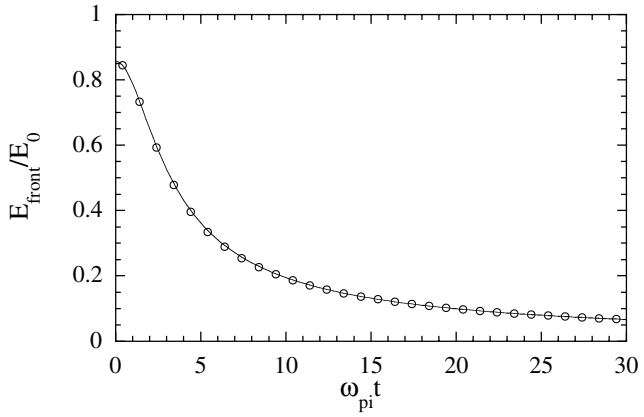

FIG. 3. Electric field at the ion front as a function of time. The empty circles correspond to the numerical results and the full line to the theoretical formula, Eq. (9). The maximum relative error is of the order of 1.3×10^{-2} for $\omega_{pi}t \simeq 5$ and is hardly seen in this picture.

solution with the same time dependence as Eq. (14), one obtains

$$n_{i,\mathrm{front}} \simeq 4n_{i0}/\omega_{pi}^2 t^2. \tag{17}$$

Spatial derivatives of the electron and ion densities at the ion front can similarly be obtained. One first easily obtains from Eqs. (1) and (7)

$$(\partial \ln n_e/\partial x)_{\mathrm{front}} = -eE_{\mathrm{front}}/k_B T_e \simeq -2/c_s t. \tag{18}$$

Now deriving (15) with respect to space and using (16), one obtains

$$\left(\frac{d}{dt} - 3\frac{d}{dt}\ln n_i\right)\left(\frac{d}{dt} - \frac{d}{dt}\ln n_i\right)\frac{\partial}{\partial x}\ln n_i = \omega_{pi}^2 \frac{\partial}{\partial x}\left(\frac{n_e - Zn_i}{n_{e0}}\right). \tag{19}$$

Then, using Eqs. (17) and (18) and looking for a solution

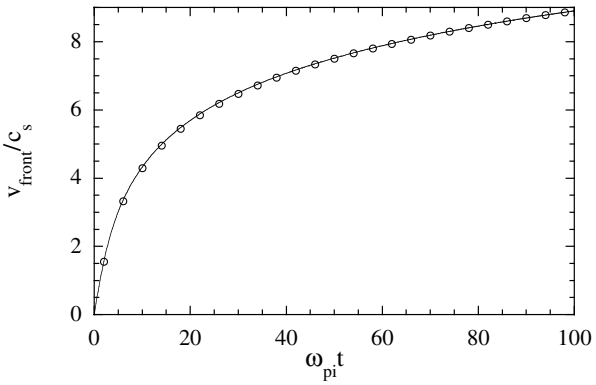

FIG. 4. Ion front velocity as a function of time. The empty circles correspond to the numerical results and the full line to the theoretical formula, Eq. (10). The maximum relative error is of the order of 7×10^{-3} for $\omega_{pi}t \simeq 9$.

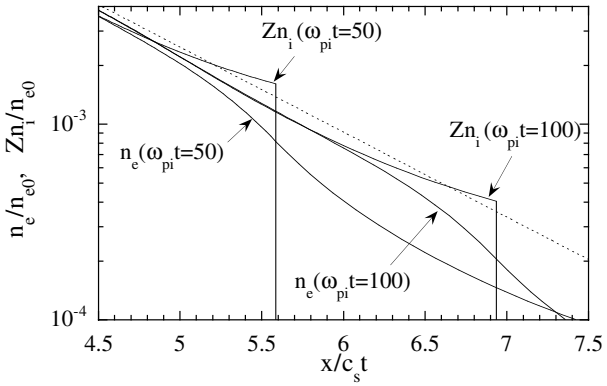

FIG. 5. Structure of the ion front at $\omega_{pi}t = 50$ and $\omega_{pi}t = 100$. The dotted line corresponds to the usual self-similar solution.

with the same time behavior as (18) one gets

$$(\partial \ln n_i/\partial x)_{\mathrm{front}} \simeq -1/2c_s t. \tag{20}$$

Time asymptotic behaviors given by Eqs. (14), (17), (18), and (20) are verified in the present numerical simulation with a high degree of precision (see Fig. 6). On the other hand these analytical results contradict the ion peak observed in the numerical solutions presented in [13,18]. (In [20] the ion peak is due to a different initial condition, i.e., an ion front extending on a few Debye lengths at time $t = 0$.)

Of crucial importance is the energy spectrum of the ions deduced from the model. The self-similar model predicts a number of ions per unit energy and unit surface given by

$$dN/d\mathcal{E} = (n_{i0}c_s t/\sqrt{2\mathcal{E}\mathcal{E}_0})\exp(-\sqrt{2\mathcal{E}/\mathcal{E}_0}), \tag{21}$$

where $\mathcal{E}_0 = Zk_B T_e$. Figure 7 shows the spectrum for $\omega_{pi}t = 30$ and $\omega_{pi}t = 100$. The cutoff energy $\mathcal{E}_{\max}$ is easily deduced from (12) for $\omega_{pi}t \gg 1$,

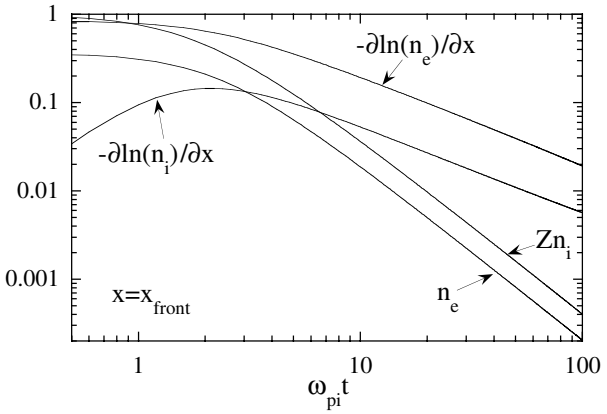

FIG. 6. Electron and ion densities, and their logarithmic derivatives at the ion front, as functions of time. Densities are normalized to n_{e0} and length to λ_{D0}.

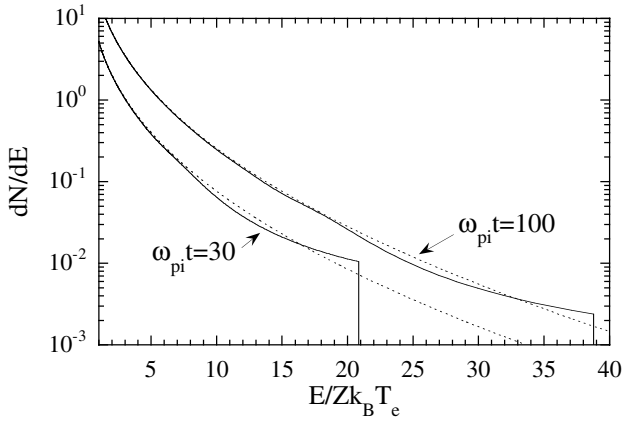

FIG. 7. Energy spectrum per unit surface at $\omega_{pi}t = 30$ and $\omega_{pi}t = 100$. Energy is normalized to Zk_BT_e, and the number of ions per unit surface and unit energy is normalized to $n_{i0}\lambda_{D0}/Zk_BT_e$. The dotted lines correspond to the prediction of the self-similar solution, Eq. (21).

$$\mathcal{E}_{\max} \simeq 2\mathcal{E}_0[\ln(2\tau)]^2. \tag{22}$$

In summary we have established accurate results for the structure of the ion front of a plasma expanding freely into a vacuum. The resultant ion energy spectrum is determined and a precise expression for its cutoff is given. In the interpretation of a real experiment additional effects may have to be taken into account, such as non-Maxwellian electron distribution function [14,15,17,19,24], electron recirculation in thin foils [9], electron temperature time dependence [17], 2D and 3D effects [6,21], magnetic field effects [3,22], non-Boltzmann equilibrium [15,16], effect of a finite initial ion density gradient [7,11,21], ionization mechanisms [10], etc.

The author acknowledges the fruitful comments of P. Audebert and S. Hüller. This work was supported in part by INTAS Project No. 01-233.

[1] K. Krushelnick *et al.*, Phys. Plasmas **7**, 2055 (2000).
[2] S. P. Hatchett *et al.*, Phys. Plasmas **7**, 2076 (2000).
[3] E. L. Clark *et al.*, Phys. Rev. Lett. **84**, 670 (2000).
[4] A. Maksimchuk *et al.*, Phys. Rev. Lett. **84**, 4108 (2000).
[5] E. L. Clark *et al.*, Phys. Rev. Lett. **85**, 1654 (2000).
[6] R. A. Snavely *et al.*, Phys. Rev. Lett. **85**, 2945 (2000).
[7] A. J. Mackinnon *et al.*, Phys. Rev. Lett. **86**, 1769 (2001).
[8] J. Badziak *et al.*, Phys. Rev. Lett. **87**, 215001 (2001).
[9] A. J. Mackinnon *et al.*, Phys. Rev. Lett. **88**, 215006 (2002).
[10] M. Hegelich *et al.*, Phys. Rev. Lett. **89**, 085002 (2002).
[11] M. Roth *et al.*, Phys. Rev. ST Accel. Beams **5**, 061301 (2002).
[12] A.V. Gurevich, L.V. Pariiskaya, and L. P. Pitaevskii, Zh. Eksp. Teor. Fiz. **49**, 647 (1965) [Sov. Phys. JETP **22**, 449 (1966)].
[13] J. E. Crow, P. L. Auer, and J. E. Allen, J. Plasma Phys. **14**, 65 (1975).
[14] J. S. Pearlman and R. L. Morse, Phys. Rev. Lett. **40**, 1652 (1978).
[15] J. Denavit, Phys. Fluids **22**, 1384 (1979).
[16] P. Mora and R. Pellat, Phys. Fluids **22**, 2300 (1979).
[17] M. A. True, J. R. Albritton, and E. A. Williams, Phys. Fluids **24**, 1885 (1981).
[18] A.V. Gurevich and A. P. Meshcherkin, Zh. Eksp. Teor. Fiz. **53**, 1810 (1981) [Sov. Phys. JETP **53**, 937 (1981)].
[19] Y. Kishimoto *et al.*, Phys. Fluids **26**, 2308 (1983).
[20] C. Sack and H. Schamel, Phys. Rep. **156**, 311 (1987).
[21] S. C. Wilks *et al.*, Phys. Plasmas **8**, 542 (2001).
[22] A. Pukhov, Phys. Rev. Lett. **86**, 3562 (2001).
[23] H. Ruhl *et al.*, Fiz. Plazmy **27**, 387 (2001) [Plasma Phys. Rep. **27**, 363 (2001)]
[24] V. F. Kovalev, Yu. Bychenkov, and V.T. Tikhonchuk, Zh. Eksp. Teor. Fiz. **122**, 264 (2002) [Sov. Phys. JETP **95**, 226 (2002)].